HHS Public Access

Author manuscript

Acta Biomater. Author manuscript; available in PMC 2020 June 01.

Published in final edited form as:

Acta Biomater. 2019 June ; 91: 186–194. doi:10.1016/j.actbio.2019.04.049.

Synergistic Effects of Laminin-1 Peptides, VEGF and FGF9 on Salivary Gland Regeneration

Kihoon Nam[1], **Spencer M. Dean**[1], **Callie T. Brown**[1], **Randall J. Smith Jr.**[3], **Pedro Lei**[2], **Stelios T. Andreadis**[2,3,4,*], and **Olga J. Baker**[1,*]

[1]School of Dentistry, The University of Utah, Salt Lake City, Utah 84108, United States

[2]Department of Chemical and Biological Engineering, University at Buffalo, The State University of New York, Buffalo, New York 14260, United States

[3]Department of Biomedical Engineering, School of Engineering and Applied Sciences, University at Buffalo, The State University of New York, Buffalo, New York 14260, United States

[4]Center of Bioinformatics and Life Sciences, University at Buffalo, The State University of New York, Buffalo, New York 14260, United States

Abstract

Hyposalivation is associated with radiation therapy, Sjogren's syndrome and/or aging, and is a significant clinical problem that decreases oral health and overall health in many patients and currently lacks effective treatment. Hence, methods to regenerate salivary glands and restore saliva secretion are urgently needed. To this end, this study describes the modification of fibrin hydrogels with a combination of laminin-1 peptides (YIGSR and A99) and human growth factors (vascular endothelial growth factor and fibroblast growth factor 9) to enhance regeneration in a salivary gland injury mouse model. Our results indicate that these fortified hydrogels enhanced angiogenesis and neurogenesis while promoting formation of acinar structures, thereby leading to enhanced saliva secretion. Such functional recovery indicates salivary gland regeneration and suggests that our technology may be useful in promoting gland regeneration and reversing hyposalivation in a clinical setting.

Graphical Abstract

[*]co-corresponding authors: Stelios T. Andreadis, Ph.D. sandread@buffalo.edu, Olga J. Baker, D.D.S., Ph.D. olga.baker@hsc.utah.edu.

Declarations of interest

KN, SMD, CTB, RJS, PL, STA and OJB declare no conflicts of interest.

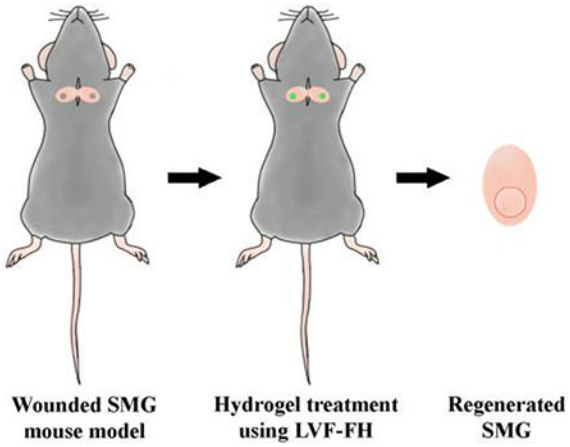

Keywords

Biomaterial; hydrogel; scaffold; regeneration; extracellular matrix; tissue engineering; saliva; salivary glands

1. Introduction

Reduced saliva secretion also known as hyposalivation, is a significant clinical concern that decreases oral health and overall health in many patients [1, 2]. Specifically, patients suffering with this condition are predisposed to microbial infections, have difficulty in chewing and swallowing food, and experience oral discomfort thereby reducing their quality of life [3]. Hyposalivation may have different causes including radiation therapy, Sjogren's syndrome (SS) and aging [4, 5]. Efficient therapeutic strategies are urgently needed to improve salivary gland regeneration in patients suffering from hyposalivation [6, 7].

The combination of two growth factors (GFs), vascular endothelial growth factor (VEGF) and fibroblast growth factor 9 (FGF9) have been shown to play a critical role in promoting vascularization and nerve formation in different organs [8, 9]. Specifically, VEGF improves tissue vascularization and thereby regeneration in a variety of tissues including skin, bone, heart, cornea [10, 11]. On the other hand, FGF9 was shown to support vascularization by attracting smooth muscle cells that stabilize the newly formed microvasculature [9, 12]. Moreover, FGF9 is expressed in neurons and has been shown to play important physiological functions including establishing and maintaining cortical circuits [13], promoting glial cell development and enhancing motoneuron survival [14–16]. Recently, we showed that the combination of VEGF and FGF9 in a fibrin hydrogel (FH)-based release system significantly enhanced neovascularization and promoted ectopic bone formation *in vivo* [9].

Our previous studies demonstrated that laminin-1 peptides (L_{1p}) conjugated to FH (L_{1p}-FH) induce acinar-like formation *in vitro* as well as submandibular gland (SMG) regeneration in a mouse wound model [17–19]. The regenerated SMG displayed both structural and functional recovery close to that observed in healthy controls. However, neovascularization and innervation were inefficient and might have contributed to the low acinar-to-ductal cell

ratio in experimental (1:1) vs. sham control animals (2.6:1), possibly compromising long-term tissue homeostasis [20, 21]. To address this challenge, we examined whether conjugation of VEGF and FGF9 in the L_{1p}-FH (LVF-FH) could enhance neovascularization and innervation, thereby increasing gland regeneration *in vivo*.

2. Materials and Methods

2.1. Materials

Lyophilized human fibrinogen and Millex syringe filter were purchased from EMD Millipore (Billerica, MA). Lyophilized bovine thrombin, calcium chloride and ε-aminocaproic acid (εACA) were purchased from Sigma-Aldrich (St. Louis, MO). Sulfosuccinimidyl 6-(3'-(2-pyridyldithio)propionamido)hexanoate (Sulfo-LC-SPDP) was purchased from Thermo Fisher Scientific (Newington, NH). Human Factor XIII was purchased from Enzyme Research Laboratories (South Bend, IN). Dialysis membrane was purchased from Spectrum Laboratories (Rancho Dominguez, CA). Picrosirius red staining was purchased from Abcam (Cambridge, MA). TO-PRO-3 iodide, Alexa Fluor 488 conjugated anti-rabbit IgG secondary antibody and Alexa Fluor 568 conjugated anti-mouse IgG secondary antibody were purchased from Invitrogen (Carlsband, CA). Rabbit anti-aquaporin 5, mouse anti-cytokeratin 7, rabbit anti-Ki-67, mouse anti-ICAM-1, rabbit anti-N-cadherin and mouse anti-beta III tubulin were purchased from Abcam. Rabbit anti-VCAM-1 was purchased from Cell Signaling Technology (Danvers, MA). Peptides were synthesized by University of Utah DNA/Peptide synthesis core facility. Female C57BL/6 mice at 6 weeks old weighing 15–19 g were purchased from the Jackson Laboratory (Bar Harbor, ME).

2.2. Animals

Eighty-eight female mice were randomly distributed into 8 groups: treated without scaffold, with FH, with VF-FH (VEGF and FGF9 conjugated FH), with L_{1p}-FH, with LV-FH (VEGF conjugated L_{1p}-FH), with LF-FH (FGF9 conjugated L_{1p}-FH), with LVF-FH (VEGF and FGF9 conjugated L_{1p}-FH), and sham control. For these studies, animals were housed in cages in a room with a controlled environment (12 h day/night cycles) and provided with a standard pellet diet and water. Additionally, all animal management, anesthesia, and surgeries were performed in compliance with the ARRIVE guidelines and an approved University of Utah Institutional Animal Care and Use Committee protocol. Finally, Carprofen (5 mg/kg/day) was used to manage incision-induced pain after surgery.

2.3. Hydrogel preparation

Peptide conjugated FH was created following the method reported previously [17]. Briefly, peptides derived from L1 (A99: CGGALRGDN-amide, YIGSR: CGGADPGYIGSRGAA-amide) were synthesized on a peptide synthesizer using a standard Fmoc solid-phase peptide synthesis with a cysteine and two glycine residues (Cys-Gly-Gly) at the N-terminus. Then, peptides were purified using reverse-phase HPLC and high-purity peptides (>98%) were used for conjugation. To make peptide conjugated fibrinogen, fibrinogen was activated using small cross linker, Sulfo-LC-SPDP. Then, activated fibrinogen was chemically conjugated with the free thiol group of cysteine residues. The reaction yield was approximately 80% for

A99 conjugated FH (350 ± 3.70 kDa) and 90% for YIGSR conjugated FH (347 ± 2.98 kDa). Thin layer chromatography and ultraviolet-visible spectroscopy were used to monitor the reactions, and static light scattering method and gel permeation chromatography were used to determine the molecular weight. Finally, the product was dialyzed, lyophilized and stored at −80 °C until use. Human VEGF165 and FGF9 were covalently conjugated into FH through the action of factor XIII (FXIII). To this end, the FXIII recognition sequence, NQEQVSP was added downstream of a histidine tag at the N-terminus of each GF and the resulting fusion proteins were termed NQ-VEGF and NQ-FGF9, respectively. The yields from *E. coll* cultures were approximatively 5 to 10 mg/L of culture for NQ-VEGF and 10 to 20 mg/L of culture for NQ-FGF9 [9]. GFs were also stored at −80 °C until use. Subsequently, hydrogels were prepared by mixing each component in Tris-buffered saline (TBS) with $CaCl_2$ (2.5 mM) and εACA, which inhibits plasmin mediated fibrin gel degradation. Note that FH degrades after eight days with the GF being release within that time frame [19]. Scaffold conditions are summarized in Table 1.

2.4. Animal model

The SMG wound model was created following the method reported previously [18, 19]. Briefly, C57BL/6 mice were anesthetized with 3% isoflurane and 0.5 cm skin incision was made along the anterior surface of the neck. Mouse SMGs were exposed and the surgical wounds were created using a 3-mm diameter biopsy punch (Supplementary video). The percentage loss of SMG was 20.03 ± 4.72 % (w/w). Then, 20 μL of each hydrogel formulation (as indicated in Table 1) was injected into each wound. An aluminum plate was placed underneath for 15 seconds to prevent hydrogel leakage. Finally, the skin incision was sutured and mice were housed in cages in a room with a controlled environment for 20 days.

2.5. Measurement of body weight

Decreased body weight has been correlated with insufficient saliva secretion, given that the latter causes difficulties in eating and subsequent malnutrition [22, 23]. Therefore, post-surgery body weight was monitored as a means to quantify this factor. Mice were weighed at the start of each experiment and data was collected for 20 days. Then, statistical significance was assessed by two-way ANOVA ($p < 0.05$) and Dunnett's post-hoc test for multiple comparisons to the untreated group.

2.6. Saliva flow rate

Mice were anesthetized with ketamine (100 mg/kg) and xylazine (5 mg/kg), and injected with pilocarpine (50 mg/kg) and isoproterenol (0.5 mg/kg) via intraperitoneal injection to stimulate saliva secretion after 20 days. Then, whole saliva was collected using a micropipette for 5 min. Total saliva flow rate was measured based on the following formula:

$$\text{Saliva flow rate} = \frac{\text{Volume of stimulated saliva (μL)}}{\text{Body weight (g)} \times \text{collection time (min)}}$$

Finally, statistical significance was assessed by one-way ANOVA ($p < 0.05$) and Dunnett's post-hoc test for multiple comparisons to the untreated group and sham control group.

2.7. Histological study

After 20 days, SMGs were immersed in 10% formalin at room temperature for overnight, dehydrated in 70% ethanol solution, embedded in paraffin and cut longitudinally into 5 μm sections that included the wound and flanking unwounded tissue. SMG sections were deparaffinized with xylene and rehydrated with serial ethanol solutions (100%, 95%, 80%, 70% and 50%) and distilled water. Then, picrosirius red staining were performed, and specimens were examined in the regenerating neo-tissue and surrounding control tissue using a Leica DMI6000B inverted microscope (Leica Microsystems, Wetzlar, Germany).

2.8. Confocal microscopy

Deparaffinized sections were incubated in sodium citrate buffer (10 mM sodium citrate, 0.05% Tween 20, pH 6.0) at 95 °C for 30 min for antigen retrieval. Then, sections were washed with distilled water, and permeabilized with 0.1% Triton X-100 in PBS at room temperature for 45 min. Sections were blocked in 5% goat serum in PBS for 1 h at room temperature and incubated for overnight at 4°C with primary antibody solution as described in Table 2. The following day, specimens were washed three times with PBS and incubated with secondary antibody solution (Table 2) for 1 h at room temperature. Sections were then washed three times with PBS and counter-stained with TO-PRO-3 iodide at room temperature for 15 min (1:1000 dilution). Finally, regenerating areas from the various specimens were analyzed using a confocal Zeiss LSM 700 microscope using a 20× objective. In addition, the ratio of acinar structures to ductal structures was analyzed using ImageJ and GraphPad Prism 6.

3. Results

3.1. LVF-FH sustain animal weight post-surgery

We engineered fusion proteins of each GF with the NQEQVSP peptide, which is a substrate of FXIIIa. During fibrin polymerization, FXIIIa recognizes NQEQVSP and incorporates NQEQVSP-VEGF, NQEQVSP-FGF9 or both into the FH. Therefore, the GFs are enzymatically conjugated into the hydrogels, which polymerize very rapidly (less than 1 min) on the wound site, providing a substrate for cell migration and wound closure. Since the GFs are conjugated, they are not released by diffusion but only degradation of FH. This is why we termed this mode of delivery, cell-controlled GF release [9, 24]. It is well known that saliva quantity and quality is important for eating, swallowing and digestion while compromising saliva production can lead to significant reduction in body weight due to reduced caloric intake [19, 25]. To evaluate whether LVF-FH could improve glandular function, we measured the body weight of mice receiving the indicated treatments for 20 days after surgery. Our results demonstrated that mouse body weight within the LVF-FH treatment group was similar to the group treated with L_{1p}-FH or the sham control and significantly higher than the group treated with FH alone or the untreated control (Fig. 1).

3.2. Cell proliferation is not affected by the presence of GFs in the FH

While cell proliferation is required for tissue regeneration, uncontrolled and abnormal growth of cells for a long time is a hallmark of cancer and it plays a vital role in tumor

development and progression [26]. Therefore, we examined cell proliferation of all treated group using Ki-67, which is widely used as cell proliferation indicator. As shown in Fig. 2 the regenerated areas within all experimental groups were similar to sham controls on day 20 post-surgery, indicating that the presence of peptides and GFs does not cause abnormal proliferation (note that images A-G correspond to wounded regenerating areas).

3.3. LVF-FH promoted collagen production and organization

To determine whether LVF-FH promoted healing of SMG, we stained the SMG tissue sections with hematoxylin and eosin. As shown in Fig. 3, LVF-FH treated samples displayed almost complete wound closure and organized structure similar to sham controls.

Next, we determined collagen deposition as a function of regenerating treatment. Similar to previous studies [18, 19], we observed areas of intense red staining consistent with irregular collagen deposition (yellow arrows), interspersed with white spaces indicating absence of collagen deposition at the interlobular spaces (green arrows) in untreated and FH-treated samples (Fig. 4A–B). On the other hand, in VF-FH and L_{1p}-FH-treated samples we detected thick intense red staining surrounding the intact interlobular areas consistent with irregular collagen deposition (yellow arrows) surrounding white to light pink spaces at the intralobular areas consistent with enhanced acinar and ductal lumens (blue arrows) (Fig. 4C–D). Finally, in LV-FH, LF-FH and LVF-FH we observed a fine red lining around the interlobular areas consistent with organized collagen deposition (white arrows) surrounding narrow light pink spaces consistent with well-developed acinar and ductal lumens similar to sham controls (Fig. 4E–G).

3.4. LVF-FH promoted regeneration of acinar structures

Next, we examined the expression of SG structural and functional markers, aquaporin 5 (AQP5, water channel protein, acinar marker, Fig.5; green) and cytokeratin 7 (K7, ductal epithelial marker, Fig. 5; red), in the regenerating areas (*i.e.* the areas where new tissue was formed). As shown in Fig. 5, the groups treated with FH, VF-FH, LV-FH or LF-FH showed little to no AQP5 staining (Fig. 5B–C, E–F). Moreover, the limited AQP5 staining in these groups was confined to areas close to the unwounded sites (while AQP5 staining was present in the unwounded areas from untreated controls; data not shown). In contrast, both L_{1p}-FH and LVF-FH treated groups showed high intensity of AQP5 apical signal. While L_{1p}-FH-treated groups showed organized AQP5 apical localization only in clustered areas (Fig. 5D), the LVF-FH treated groups showed a more uniform distribution and apical localization of AQP5 across the tissue (Fig. 5G) that was comparable to sham control (Fig. 5H, I, $p = 0.0267$). Furthermore, SMG treated with LVF-FH was the only treatment group displaying similar ratio of acinar to ductal structures (2.1:1) as compared to sham control (2.6:1, $p = 0.0376$, Fig. 5J). Note that that L1 was critical for improving cell organization *e.g.*, cell attachment and cell migration, [27]) while GFs are critical for promoting blood vessels and nerve growth [8, 9]. Moreover, it is interesting to mention that the groups treated with GFs alone or in combination show more ductal structures (*i.e.*, red staining in Fig. 5).

3.5. LVF-FH enhanced angiogenesis in healing SMG tissues

In order to evaluate angiogenesis, specimens were immunostained for VCAM-1 (Fig 6; green) and ICAM-1 (Fig. 6; red). We found that wounds treated with FH alone (Fig. 6B) displayed no staining for any of the blood vessel markers in regenerated tissue areas, similar to untreated controls (Fig. 6A). Fibrin containing VEGF and FGF9 (VF-FH) displayed weak staining for VCAM-1 but no staining for ICAM-1 (Fig. 6C). L_{1p}-FH displayed weak and disorganized signals for both ICAM-1 and VCAM-1 (Fig. 6D). Combination of laminin-1 peptide conjugated FH and VEGF (LV-FH) increased ICAM-1, while the VCAM-1 signal remained low (Fig. 6E). On the other hand, FGF9 in L_{1p}-FH (LF-FH) showed no staining for either marker, suggesting that FGF9 alone had no effect on angiogenesis (Fig. 6F). Interestingly, the group treated with LVF-FH (Fig. 6G) displayed a strong co-localized signal for VCAM-1 and ICAM-1 similar to sham controls (Fig. 6H), indicating that VEGF and FGF9 worked synergistically with the laminin-1 peptides to increase angiogenesis in the regenerated gland. Finally, VCAM-1 and ICAM-1 staining was present in the unwounded areas from untreated controls (data not shown).

3.6. LVF-FH enhanced gland innervation during regeneration

We also determined the number and distribution of newly formed nerves within the regenerating gland by immunostaining for N-cadherin (Fig 7; green) and beta III tubulin (Fig. 7; red). Our results showed weak and disorganized expression for neuronal markers in SMG treated with FH, VF-FH or untreated controls (Fig. 7A–C). In contrast, L1p-FH treated groups showed high expression of punctate N-cadherin around acinar and ductal areas (Fig. 7D). Similarly, beta III tubulin showed organized expression around these areas. Surprisingly, addition of VEGF (LV-FH) or FGF9 (LF-FH) alone showed less staining for N-cadherin (Fig. 7E, F). On the other hand, the combination of VEGF and FGF9 in the presence of laminin-1 peptides (LVF-FH) showed high expression of N-cadherin as well as beta III tubulin (Fig. 7G). Finally, N-cadherin as well as beta III tubulin staining was present in the unwounded areas from untreated controls (data not shown). Collectively, these results indicate that laminin-1 peptides, VEGF and FGF9 work synergistically to promote innervation of the newly formed gland tissues.

3.7. LVF-FH restored salivary function in regenerated glands

Saliva secretion is the main function of SMG and a reliable indicator of salivary gland regeneration [28]. Since LVF-FH promoted angiogenesis and innervation of healing glands we hypothesized that the newly regenerated glands might have recovered salivary function. To address this hypothesis, we measured saliva flow rates in the indicated groups. As shown in Fig 8, the saliva secretion rate from the groups treated with fibrin hydrogels containing laminin-1 peptides (L_{1p}-FH) was significantly higher as compared to the FH-treated or untreated group. While addition of either FGF9 or VEGF alone had no additional effect, the combination of FGF9 and VEGF with L_{1p} increased saliva secretion even further, to a similar level as sham controls ($p = 0.2493$). These results indicate that the combination of L_{1p}, VEGF and FGF9 restored saliva secretion in the newly formed glands to the level of unwounded healthy controls.

4. Discussion

The primary goal of this study was to determine whether L_{1p}-FH regenerative effects are enhanced by the addition of the GF involved in blood vessel and nerve formation (*i.e.*, VEGF and FGF9). Our previous studies demonstrated that L_{1p}-FH enhances wound healing while improving saliva secretion in a wounded SMG mouse model [18, 19]. However, the acinar-to-ductal ratio was low and both angiogenesis and innervation were limited [19]. Taken together, these results suggested that while laminin-1 peptides promoted wound healing, additional factors might be necessary for enhanced gland regeneration. To this end, we employed a combination of VEGF and FGF9, which were previously shown to enhance angiogenesis [9]. VEGF and FGF9 were also shown to have an effect on neurogenesis [12, 29–31] and its receptors (FGFR1–3) [32] induces epithelial budding and duct elongation in *ex vivo* SMG organ cultures [33]. Our results are consistent with previous studies showing that VEGF promotes blood vessel growth in a number of tissues [34–37] and that FGF9 stabilizes the newly formed blood vessels by recruiting smooth muscle cells to the vascular wall [38]. In agreement with our previous work on bone regeneration [9], our results support the notion that enhanced neovascularization promotes functional tissue regeneration, which is accompanied by enhanced innervation [39, 40]. Notably, both angiogenesis and innervation correlated with increased saliva secretion, indicating that this scaffold combination promoted functional gland recovery. Since all components of our composite FH including fibrin, L1 peptides and GFs degrade over a period of approximately eight days [18, 19], and are effective after a single application, our formulation may provide a safe alternative for potential clinical applications. Future studies may identify additional factors that may further increase these effects and understand the mechanisms underlying the enhanced regeneration. Moreover, we will verify if there are differences in regeneration patterns as a function of sex, considering this study is limited to the use of female mice only. Finally, while our work demonstrated the effectiveness of our technology in the context of physical injury, it may also apply in other types of injury *e.g.* radiation damage of the gland, thereby providing a viable treatment for people suffering from hyposalivation.

5. Conclusion

In summary, we engineered FH to contain multiple regenerative cues including laminin-1 peptides and GFs to form functional salivary gland tissue. LVF-FH promoted salivary epithelial tissue regeneration, vascularization, neurogenesis and healing. The regenerated gland tissues displayed not only structural but also functional similarities as normal gland tissues. Our results indicate that L_{1p} and GF modified FH can be used for future therapeutic applications.

Supplementary Material

Refer to Web version on PubMed Central for supplementary material.

Acknowledgements

This research was supported by the National Institute of Dental and Craniofacial Research/National Institutes of Health (NIDCR/NIH) under the following awards: R56DE021697 (OJB), R01DE022971 (OJB and STA), R01DE027884 (OJB).

References

[1]. Vissink A, Mitchell JB, Baum BJ, Limesand KH, Jensen SB, Fox PC, Elting LS, Langendijk JA, Coppes RP, Reyland ME. Clinical management of salivary gland hypofunction and xerostomia in head and neck cancer patients: successes and barriers. International journal of radiation oncology, biology, physics 2010;78:983–91.

[2]. Carlson ER, Ord RA. Trauma and Injuries to the Salivary Glands. Salivary Gland Pathology: John Wiley & Sons, Inc; 2015 p. 409–36.

[3]. Mortazavi H, Baharvand M, Movahhedian A, Mohammadi M, Khodadoustan A. Xerostomia Due to Systemic Disease: A Review of 20 Conditions and Mechanisms. Annals of Medical and Health Sciences Research 2014;4:503–10. [PubMed: 25221694]

[4]. Villa A, Connell CL, Abati S. Diagnosis and management of xerostomia and hyposalivation. Therapeutics and Clinical Risk Management 2015;11:45–51. [PubMed: 25653532]

[5]. Yamauchi Y, Matsuno T, Omata K, Satoh T. Relationship between hyposalivation and oxidative stress in aging mice. Journal of Clinical Biochemistry and Nutrition 2017;61:40–6. [PubMed: 28751808]

[6]. Yoo C, Vines JB, Alexander G, Murdock K, Hwang P, Jun H-W. Adult stem cells and tissue engineering strategies for salivary gland regeneration: a review. Biomaterials Research 2014;18:9. [PubMed: 26331060]

[7]. Gil-Montoya J-A, Silvestre F-J, Barrios R, Silvestre-Rangil J. Treatment of xerostomia and hyposalivation in the elderly: A systematic review. Medicina Oral, Patología Oral y Cirugía Bucal 2016;21:e355–e66.

[8]. Kanda T, Iwasaki T, Nakamura S, Kurokawa T, Ikeda K, Mizusawa H. Self-secretion of fibroblast growth factor-9 supports basal forebrain cholinergic neurons in an autocrine/paracrine manner. Brain Research 2000;876:22–30. [PubMed: 10973589]

[9]. Yuan X, Smith RJ Jr., Guan H, Ionita CN, Khobragade P, Dziak R, Liu Z, Pang M, Wang C, Guan G, Andreadis S, Yang S. Hybrid Biomaterial with Conjugated Growth Factors and Mesenchymal Stem Cells for Ectopic Bone Formation. Tissue Eng Part A 2016;22:928–39. [PubMed: 27269204]

[10]. Lovett M, Lee K, Edwards A, Kaplan DL. Vascularization Strategies for Tissue Engineering. Tissue Engineering Part B, Reviews 2009;15:353–70. [PubMed: 19496677]

[11]. Johnson KE, Wilgus TA. Vascular Endothelial Growth Factor and Angiogenesis in the Regulation of Cutaneous Wound Repair. Advances in Wound Care 2014;3:647–61. [PubMed: 25302139]

[12]. Behr B, Leucht P, Longaker MT, Quarto N. Fgf-9 is required for angiogenesis and osteogenesis in long bone repair. Proceedings of the National Academy of Sciences of the United States of America 2010;107:11853–8. [PubMed: 20547837]

[13]. Huang JY, Lynn Miskus M, Lu HC. FGF-FGFR Mediates the Activity-Dependent Dendritogenesis of Layer IV Neurons during Barrel Formation. The Journal of neuroscience : the official journal of the Society for Neuroscience 2017;37:12094–105. [PubMed: 29097598]

[14]. Todo T, Kondo T, Nakamura S, Kirino T, Kurokawa T, Ikeda K. Neuronal localization of fibroblast growth factor-9 immunoreactivity in human and rat brain. Brain Res 1998;783:179–87. [PubMed: 9507114]

[15]. Alain G, Hiroshi N, Jean- Marc P, Brigitte P, Odile d. FGF9: A motoneuron survival factor expressed by medial thoracic and sacral motoneurons. Journal of Neuroscience Research 2000;60:1–9. [PubMed: 10723063]

[16]. Lin Y, Chen L, Lin C, Luo Y, Tsai RYL, Wang F. Neuron-derived FGF9 is Essential for Scaffold Formation of Bergmann Radial Fibers and Migration of Granule Neurons in the Cerebellum. Developmental Biology 2009;329:44–54. [PubMed: 19232523]

[17]. Nam K, Jones JP, Lei P, Andreadis ST, Baker OJ. Laminin-111 Peptides Conjugated to Fibrin Hydrogels Promote Formation of Lumen Containing Parotid Gland Cell Clusters. Biomacromolecules 2016.

[18]. Nam K, Wang CS, Maruyama CLM, Lei P, Andreadis ST, Baker OJ. L1 Peptide-Conjugated Fibrin Hydrogels Promote Salivary Gland Regeneration. Journal of dental research 2017;96:798–806. [PubMed: 28208029]

[19]. Nam K, Maruyama CL, Wang C-S, Trump BG, Lei P, Andreadis ST, Baker OJ. Laminin-111-derived peptide conjugated fibrin hydrogel restores salivary gland function. PLoS ONE 2017;12:e0187069. [PubMed: 29095857]

[20]. Sekiya S, Shimizu T. Introduction of vasculature in engineered three-dimensional tissue. Inflammation and Regeneration 2017;37:25. [PubMed: 29259724]

[21]. Wang Y, Yu A, Yu F-X. The Hippo pathway in tissue homeostasis and regeneration. Protein & Cell 2017;8:349–59.

[22]. Sung JM, Kuo SC, Guo HR, Chuang SF, Lee SY, Huang JJ. Decreased salivary flow rate as a dipsogenic factor in hemodialysis patients: evidence from an observational study and a pilocarpine clinical trial. Journal of the American Society of Nephrology : JASN 2005;16:3418–29. [PubMed: 16177001]

[23]. Chambers MS, Tomsett KL, Artopoulou II, Garden AS, El-Naggar AK, Martin JW, Keene HJ. Salivary flow rates measured during radiation therapy in head and neck cancer patients: A pilot study assessing salivary sediment formation. The Journal of Prosthetic Dentistry 2008;100:142–6. [PubMed: 18672129]

[24]. Geer DJ, Swartz DD, Andreadis ST. Biomimetic delivery of keratinocyte growth factor upon cellular demand for accelerated wound healing in vitro and in vivo. Am J Pathol 2005;167:1575–86. [PubMed: 16314471]

[25]. Humphrey SP, Williamson RT. A review of saliva: normal composition, flow, and function. J Prosthet Dent 2001;85:162–9. [PubMed: 11208206]

[26]. Lopez-Saez JF, de la Torre C, Pincheira J, Gimenez-Martin G. Cell proliferation and cancer. Histology and histopathology 1998;13:1197–214. [PubMed: 9810511]

[27]. Hohenester E, Yurchenco PD. Laminins in basement membrane assembly. Cell Adhesion & Migration 2013;7:56–63. [PubMed: 23076216]

[28]. Ogawa M, Oshima M, Imamura A, Sekine Y, Ishida K, Yamashita K, Nakajima K, Hirayama M, Tachikawa T, Tsuji T. Functional salivary gland regeneration by transplantation of a bioengineered organ germ. Nature Communications 2013;4:2498.

[29]. Jin K, Zhu Y, Sun Y, Mao XO, Xie L, Greenberg DA. Vascular endothelial growth factor (VEGF) stimulates neurogenesis in vitro and in vivo. Proceedings of the National Academy of Sciences of the United States of America 2002;99:11946–50. [PubMed: 12181492]

[30]. Sun Y, Jin K, Xie L, Childs J, Mao XO, Logvinova A, Greenberg DA. VEGF-induced neuroprotection, neurogenesis, and angiogenesis after focal cerebral ischemia. Journal of Clinical Investigation 2003;111:1843–51. [PubMed: 12813020]

[31]. Kang W, Hébert JM. FGF Signaling Is Necessary for Neurogenesis in Young Mice and Sufficient to Reverse Its Decline in Old Mice. The Journal of Neuroscience 2015;35:10217. [PubMed: 26180198]

[32]. Liu Y, Ma J, Beenken A, Srinivasan L, Eliseenkova AV, Mohammadi M. Regulation of Receptor Binding Specificity of FGF9 by an Autoinhibitory Homodimerization. Structure (London, England : 1993) 2017;25:1325–36.e3.

[33]. Steinberg Z, Myers C, Heim VM, Lathrop CA, Rebustini IT, Stewart JS, Larsen M, Hoffman MP. FGFR2b signaling regulates ex vivo submandibular gland epithelial cell proliferation and branching morphogenesis. Development (Cambridge, England) 2005;132:1223–34.

[34]. Gowdak LHW, Poliakova L, Li Z, Grove R, Lakatta EG, Talan M. Induction of angiogenesis by cationic lipid-mediated VEGF165 gene transfer in the rabbit ischemic hindlimb model. Journal of Vascular Surgery 2000;32:343–52. [PubMed: 10917995]

[35]. Arsic N, Zacchigna S, Zentilin L, Ramirez-Correa G, Pattarini L, Salvi A, Sinagra G, Giacca M. Vascular endothelial growth factor stimulates skeletal muscle regeneration in Vivo. Molecular Therapy 2004;10:844–54. [PubMed: 15509502]

[36]. Kleinheinz J, Stratmann U, Joos U, Wiesmann HP. VEGF-activated angiogenesis during bone regeneration. Journal of oral and maxillofacial surgery : official journal of the American Association of Oral and Maxillofacial Surgeons 2005;63:1310–6.

[37]. Zhu H, Jiang X, Li X, Hu M, Wan W, Wen Y, He Y, Zheng X. Intramyocardial delivery of VEGF165 via a novel biodegradable hydrogel induces angiogenesis and improves cardiac function after rat myocardial infarction. Heart and vessels 2016;31:963–75. [PubMed: 26142379]

[38]. Frontini MJ, Nong Z, Gros R, Drangova M, O'Neil C, Rahman MN, Akawi O, Yin H, Ellis CG, Pickering JG. Fibroblast growth factor 9 delivery during angiogenesis produces durable, vasoresponsive microvessels wrapped by smooth muscle cells. Nature Biotechnology 2011;29:421.

[39]. Hobson MI, Green CJ, Terenghi G. VEGF enhances intraneural angiogenesis and improves nerve regeneration after axotomy. Journal of anatomy 2000;197 Pt 4:591–605. [PubMed: 11197533]

[40]. Rosenstein JM, Krum JM, Ruhrberg C. VEGF in the nervous system. Organogenesis 2010;6:107–14. [PubMed: 20885857]

Statement of Significance

- We engineered Fibrin Hydrogels (FH) to contain multiple regenerative cues including laminin-1 peptides (L_{1p}) and growth factors (GF).
- L_{1p} and GF modified FH were used to induce salivary gland regeneration in a wounded mouse model.
- Treatment with L_{1p} and GF modified FH promoted salivary epithelial tissue regeneration, vascularization, neurogenesis and healing as compared to L_{1p}-FH or FH alone.
- Results indicate that L_{1p} and GF modified FH can be used for future therapeutic applications.

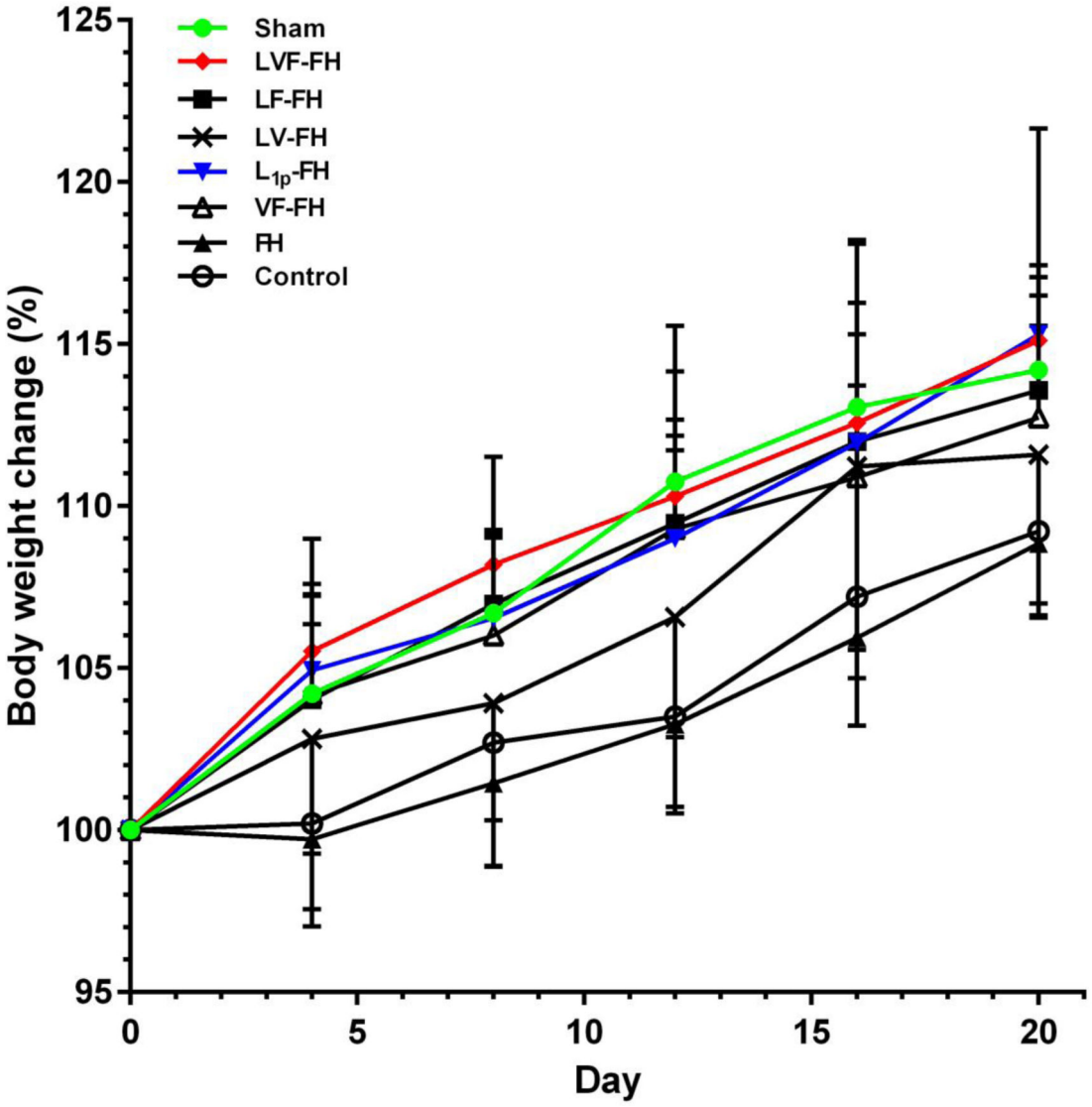

Fig. 1. LVF-FH increased body weight post-surgery.

After SMG wounding, mice received the indicated treatments and body weight was measured at the indicated times and plotted as % change in body weight over time. Data represent the means ± SD of n = 9 mice per condition and statistical significance was assessed by two-way ANOVA ($p < 0.05$) and Dunnett's post-hoc test for multiple comparisons to the untreated group are shown on Table 3.

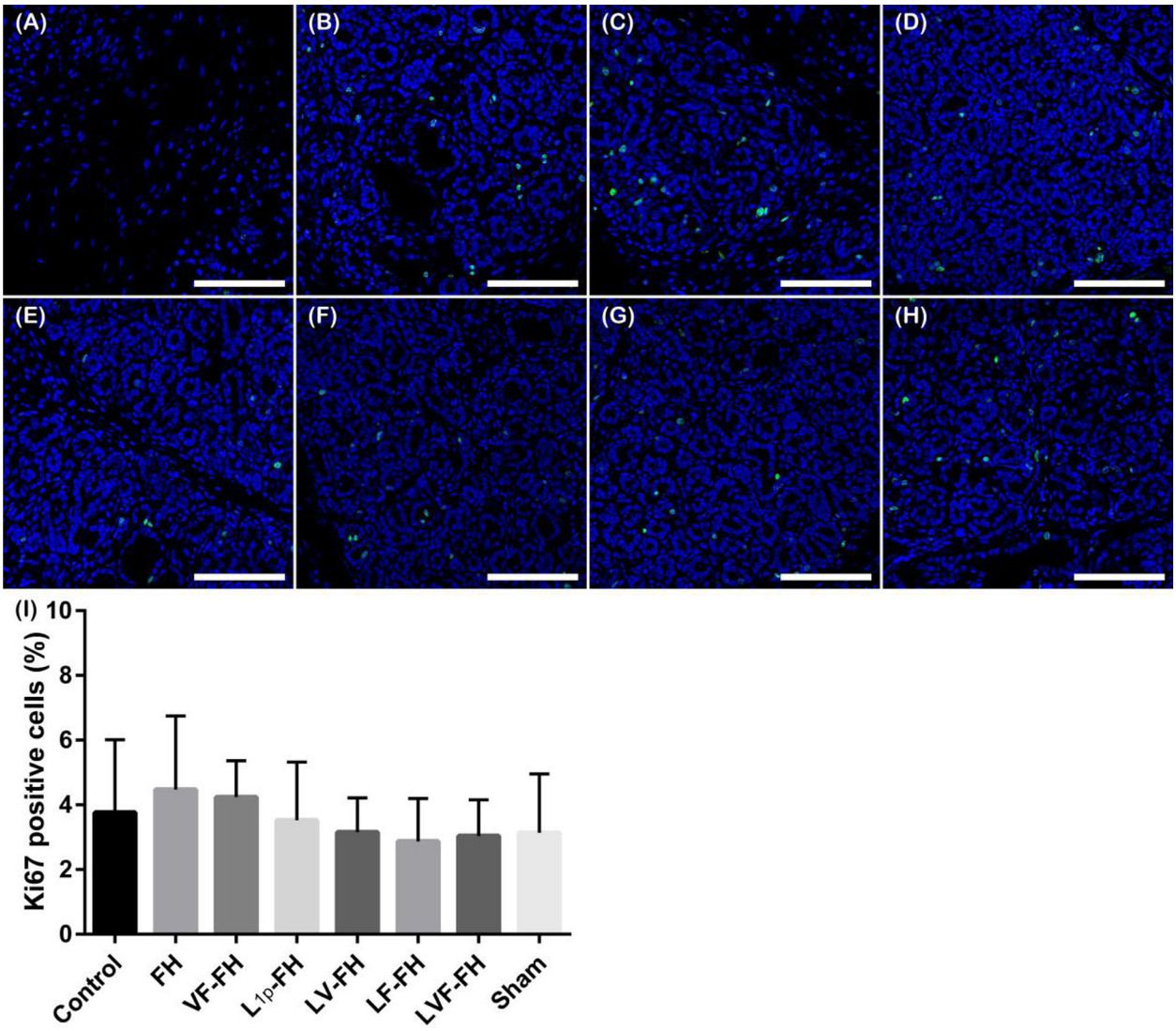

Fig. 2. Cell proliferation is similar among all indicated groups.

Immunostaining for Ki-67 (green, proliferation marker) of wounded SMG treated without scaffold (A), or with FH (B), VF-FH (C), L1p-FH (D), LV-FH (E), LF-FH (F) and LVF-FH (G). Unwounded glands served as sham controls (H). Regenerating areas were analyzed using a confocal Zeiss LSM 700 microscope at 20× magnification (bars = 100 μm). (I) The number of Ki-67^{+} cells was quantified using ImageJ and analyzed using one-way ANOVA (*$p < 0.01$, n = 12) with Tukey's multiple comparisons.

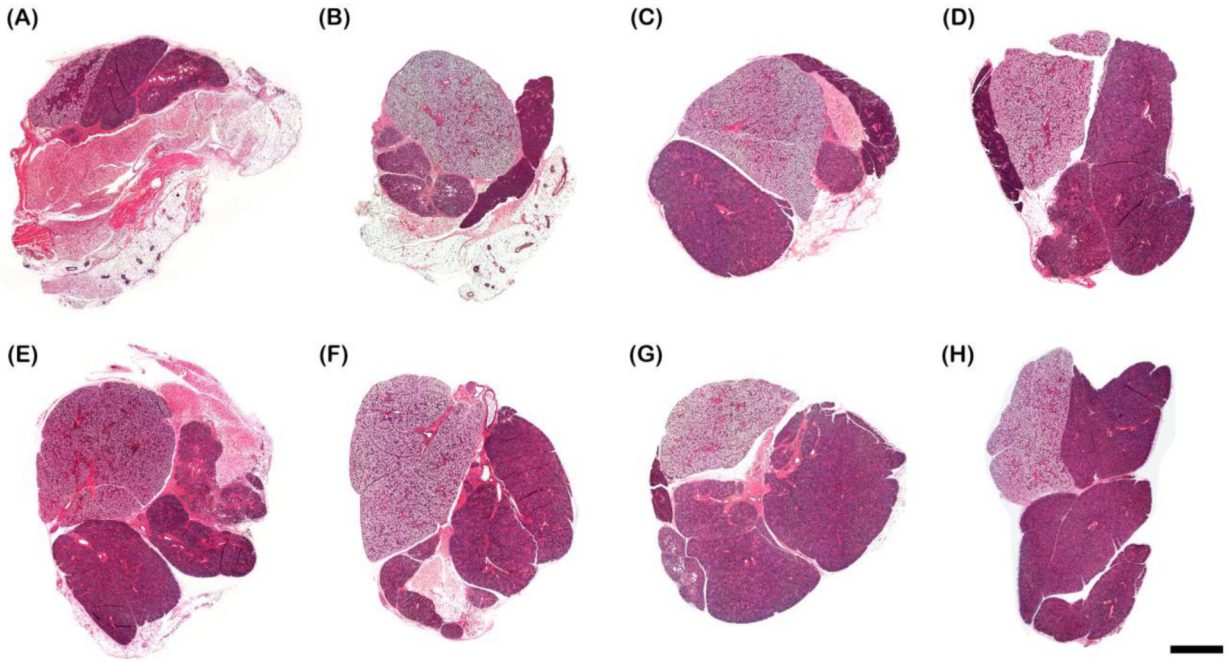

Fig. 3. LVF-FH induced wound healing.

Hematoxylin and eosin staining of wounded SMG that remained untreated (A), or treated with FH (B), VF-FH (C), L_{1p}-FH (D), LV-FH (E), LF-FH (F) and LVF-FH (G). Unwounded glands served as sham controls (H). Specimens were imaged using a Leica DMI6000B; bars = 1000 μm.

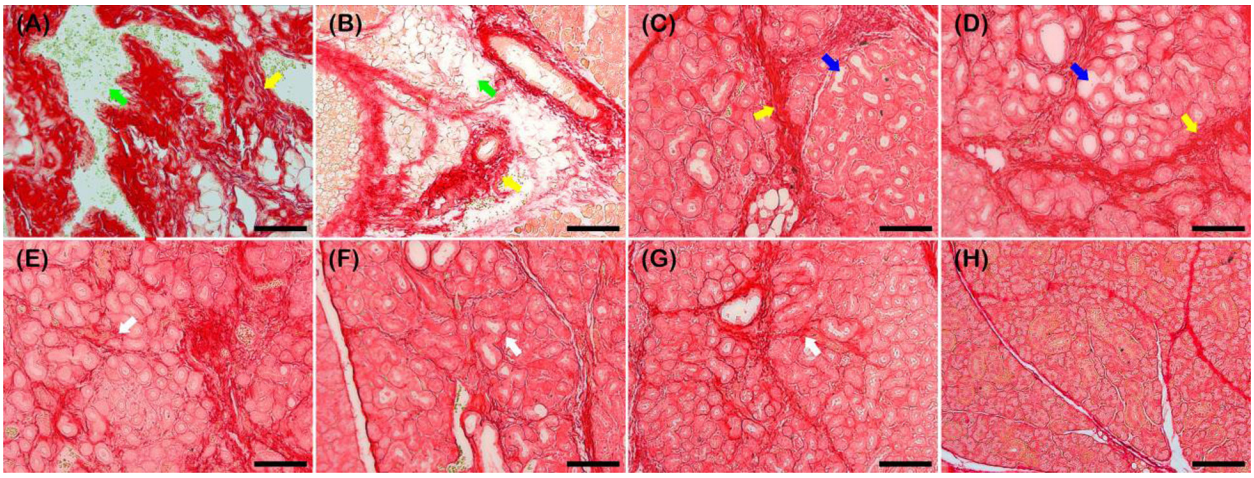

Fig. 4. LVF-FH promoted collagen production and fiber organization to a similar extent as unwounded gland tissues.

Picrosirius red staining of wounded SMG that remained untreated (A), or treated with FH (B), VF-FH (C), L_{1p}-FH (D), LV-FH (E), LF-FH (F) and LVF-FH (G). Unwounded glands served as sham controls (H). Specimens were imaged using a Leica DMI6000B; bars = 100 μm.

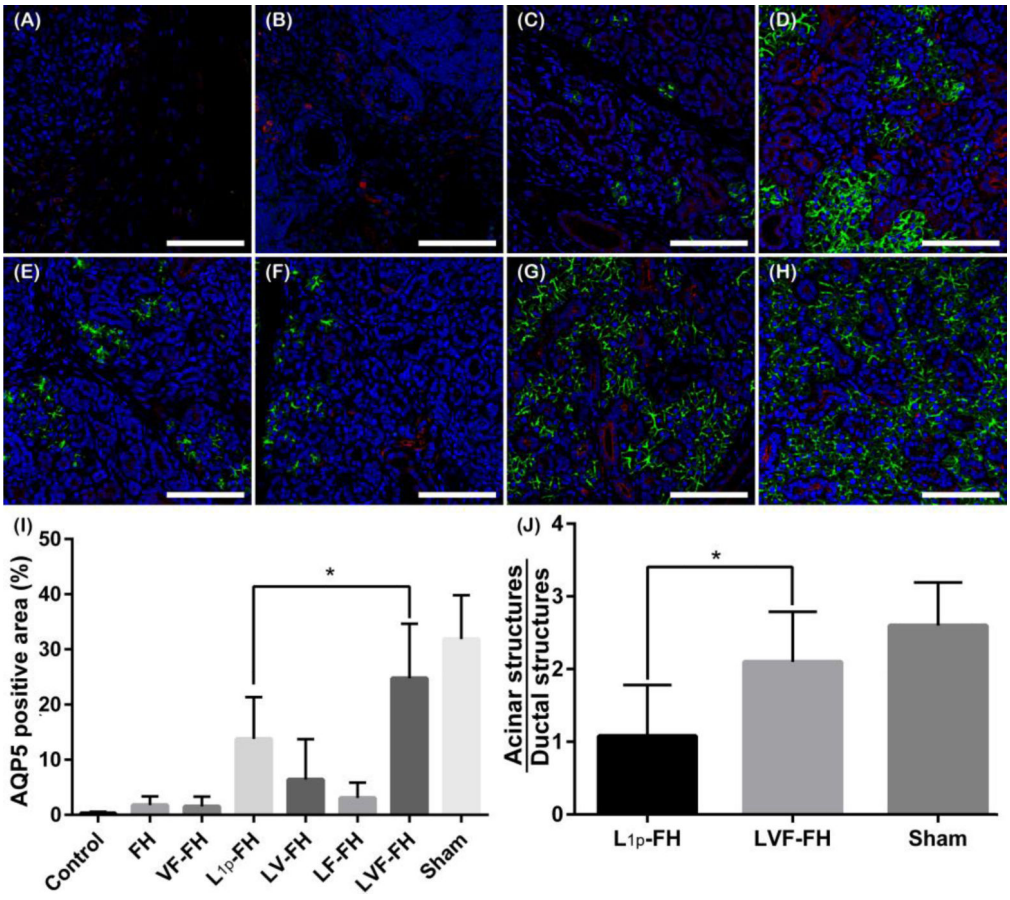

Fig. 5. LVF-FH promoted aquaporin expression throughout the newly formed glandular tissue and increased the acinar to ductal structure ratio similar to unwounded tissues.

Immunostaining for AQP5 (green, acinar marker) and K7 (red, ductal marker) in wounded SMG treated without scaffold (A), or with FH (B), VF-FH (C), L_{1p}-FH (D), LV-FH (E), LF-FH (F) and LVF-FH (G). Unwounded glands served as sham controls (H). Specimens were analyzed using a confocal Zeiss LSM 700 microscope at 40× magnification (bars = 200 μm). Positive area of AQP5 (I) and the ratio of acinar and ductal structures (J) were calculated on day 20 post-surgery using ImageJ and analyzed using one-way ANOVA (*$p < 0.01$, n = 12) and Dunnett's post-hoc test for multiple comparisons to the L_{1p}-treated group.

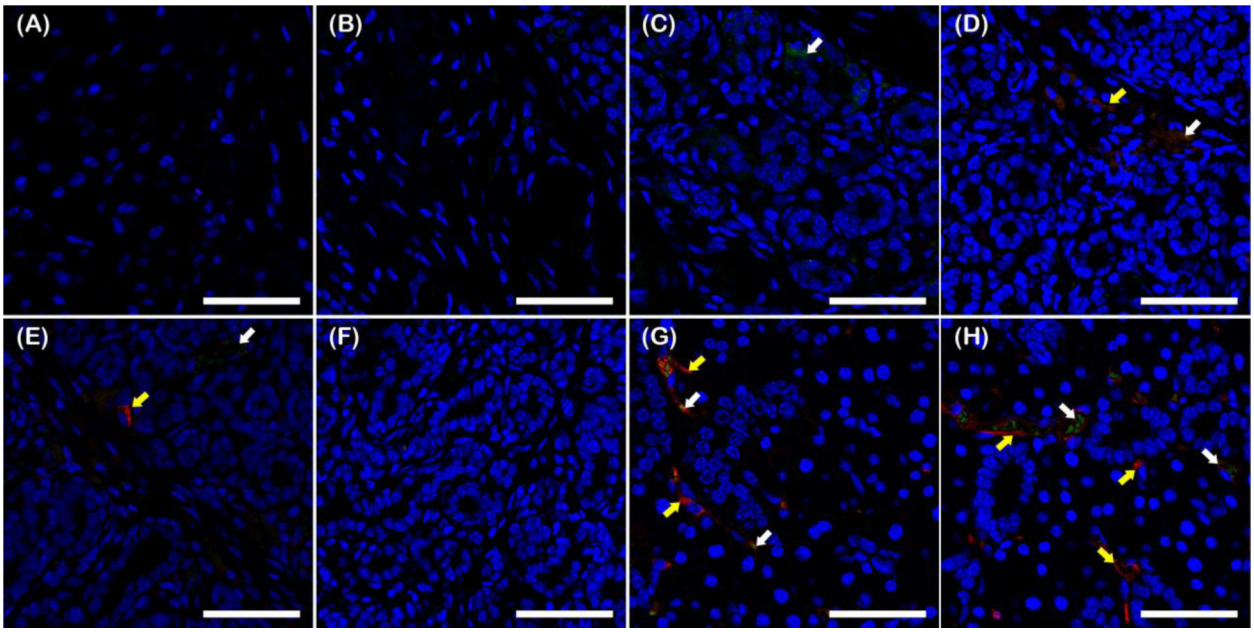

Fig. 6. LVF-FH enhanced angiogenesis in the regenerated gland tissues.

Immunostaining for VCAM-1 (green, blood vessel marker, white arrows) and ICAM-1 (red, blood vessel marker, yellow arrows) of wounded SMG treated without scaffold (A), or with FH (B), VF-FH (C), L1p-FH (D), LV-FH (E), LF-FH (F) and LVF-FH (G). Unwounded glands served as sham controls (H). Specimens were analyzed using a confocal Zeiss LSM 700 microscope at 40× magnification (bars = 200 μm).

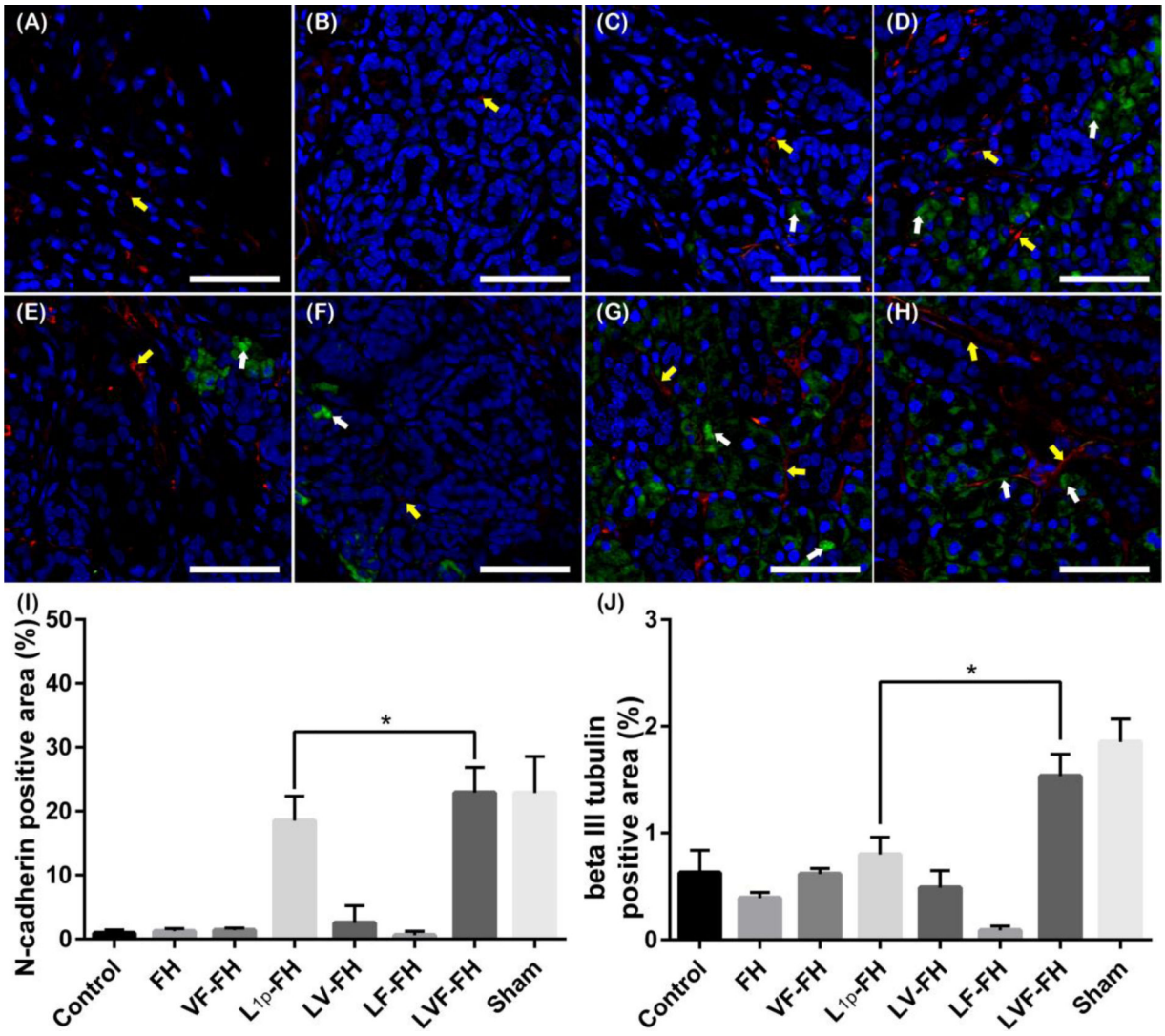

Fig. 7. LVF-FH promoted innervation of regenerated gland tissues.

Immunostaining for N-cadherin (green, neuronal marker, white arrows) and beta III tubulin (red, neuronal marker, yellow arrows) in wounded SMG tissues treated without scaffold (A), or with FH (B), VF-FH (C), L1p-FH (D), LV-FH (E), LF-FH (F) and LVF-FH (G). Unwounded glands served as sham controls (H). Specimens were analyzed using a confocal Zeiss LSM 700 microscope at 40× magnifications (bars = 200 μm). Positive area of N-cadherin (I) and beta III tubulin (J) was calculated using ImageJ and analyzed using one-way ANOVA (*$p < 0.01$, n = 12) and Dunnett's post-hoc test for multiple comparisons to the L_{1p}-treated group.

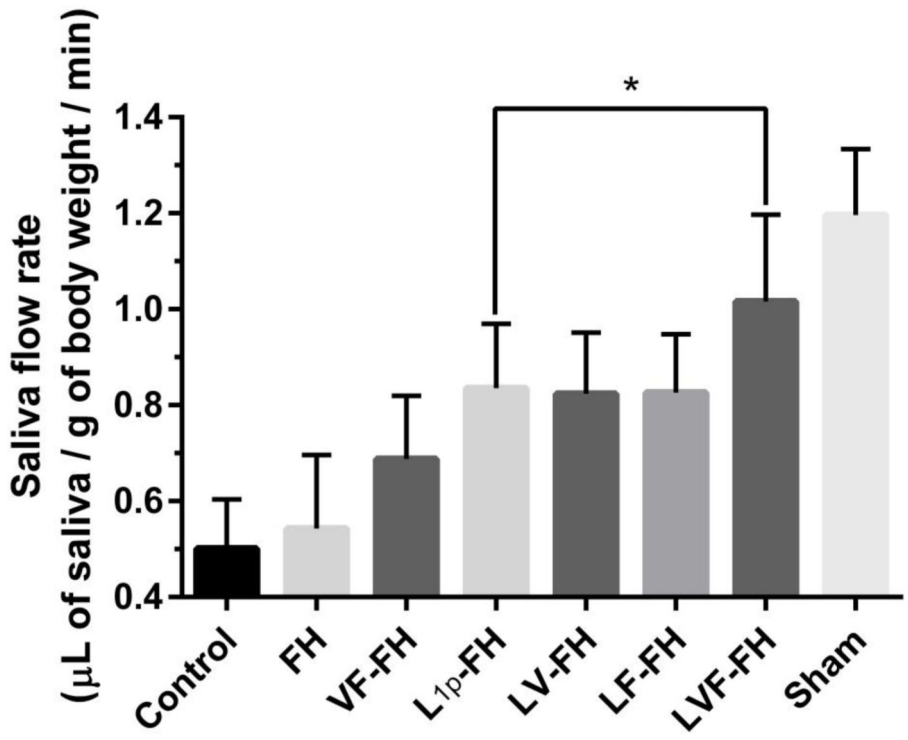

Fig. 8. LVF-FH restored saliva secretion to a similar level as unwounded glands.

Mice receiving the indicated treatments were anesthetized and stimulated with pilocarpine and isoproterenol on day 20. Then, saliva was collected for 5 min. Data represent the means ± SD of n = 8 mice per condition and statistical significance was assessed by one-way ANOVA ($p < 0.05$) and Dunnett's post-hoc test for multiple comparisons to the L_{1p}-treated group.

Table 1.

Summary of scaffold conditions

Hydrogel	Fibrinogen (mg/mL)	YIGSR-conjugated fibrinogen (mg/mL)	A99-conjugated fibrinogen (mg/mL)	FGF9 (ng/mL)	VEGF (ng/mL)	Factor XIII (PEU)	ε-ACA (mg/mL)	Thrombin (U/mL)
FH	2.5					1	2	2.5
VF-FH	2.5			100	100	1	2	2.5
L_{1p}-FH		1.25	1.25			1	2	2.5
LV-FH		1.25	1.25		100	1	2	2.5
LF-FH		1.25	1.25	100		1	2	2.5
LVF-FH		1.25	1.25	100	100	1	2	2.5

Table 2.

Antibodies used for antigen detection by immunohistochemistry

Antibody	Dilution	Company (Catalog number)
Rabbit anti-aquaporin 5	200	Abcam (ab78486)
Mouse anti-cytokeratin 7	500	Abcam (ab9021)
Rabbit anti-Ki-67	100	Abcam (ab15580)
Rabbit anti-VCAM-1	100	Cell Signaling (39036S)
Mouse anti-ICAM-1	100	Abcam(ab171123)
Rabbit anti-N-cadherin	500	Abcam (ab18203)
Mouse anti-beta III tubulin	100	Abcam (ab7751)
Alexa Fluor 488 conjugated anti-rabbit IgG	500	Invitrogen (A11008)
Alexa Fluor 568 conjugated anti-mouse IgG	200	Invitrogen (A11031)

Table 3.

p values showing a comparison between the different treatment groups with untreated control group

Group \ Day	0	4	8	12	16	20
Sham	ns	*	*	****	***	**
LVF-FH	ns	**	**	****	**	***
LF-FH	ns	ns	*	***	*	*
LV-FH	ns	ns	ns	ns	ns	ns
L_{1p}-FH	ns	*	ns	**	*	***
VF-FH	ns	ns	ns	**	ns	ns
FH	ns	ns	ns	**	ns	ns

ns = not significant;

* $p < 0.05$;

** $p < 0.01$;

*** $p < 0.001$

**** $p < 0.0001$.